analytical chemistry

TECHNICAL NOTE

pubs.acs.org/ac

Improved Precision of iTRAQ and TMT Quantification by an Axial Extraction Field in an Orbitrap HCD Cell

Peter Pichler,[*,†] Thomas Köcher,[‡] Johann Holzmann,[‡] Thomas Möhring,[§] Gustav Ammerer,[†,∥] and Karl Mechtler[‡,⊥]

[†]Christian Doppler Laboratory for Proteome Analysis, University of Vienna, Austria

[‡]Research Institute of Molecular Pathology, Vienna, Austria

[§]Thermo Fisher Scientific, Bremen, Germany

[∥]Max F. Perutz Laboratories, University of Vienna, Austria

[⊥]Institute of Molecular Biotechnology, Vienna, Austria

Supporting Information

ABSTRACT:

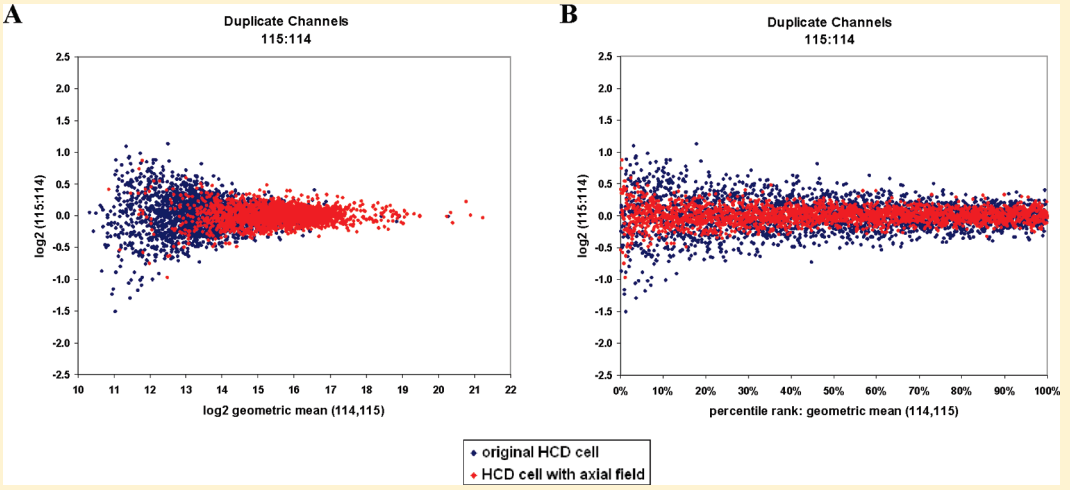

Improving analytical precision is a major goal in quantitative differential proteomics as high precision ensures low numbers of outliers, a source of false positives with regard to quantification. In addition, higher precision increases statistical power, i.e., the probability to detect significant differences. With chemical labeling using isobaric tags for relative and absolute quantitation (iTRAQ) or tandem mass tag (TMT) reagents, quantification is based on the extraction of reporter ions from tandem mass spectrometry (MS/MS) spectra. We compared the performance of two versions of the LTQ Orbitrap higher energy collisional dissociation (HCD) cell with and without an axial electric field with regard to reporter ion quantification. The HCD cell with the axial electric field was designed to push fragment ions into the C-trap and this version is mounted in current Orbitrap XL ETD and Orbitrap Velos instruments. Our goal was to evaluate whether the purported improvement in ion transmission had a measurable impact on the precision of MS/MS based quantification using peptide labeling with isobaric tags. We show that the axial electric field led to an increased percentage of HCD spectra in which the complete set of reporter ions was detected and, even more important, to a reduction in overall variance, i.e., improved analytical precision of the acquired data. Notably, adequate precision of HCD-based quantification was maintained even for low precursor ion intensities of a complex biological sample. These findings may help researchers in their design of quantitative proteomics studies using isobaric tags and establish HCD-based quantification on the LTQ Orbitrap as a highly precise approach in quantitative proteomics.

Developments in shotgun proteomics technology have focused on improving the sensitivity, mass accuracy, and speed of mass spectrometers.[1−4] However, as mass spectrometry turns quantitative,[5,6] optimizing analytical strategies for high precision and low measurement variability (i.e., low standard deviation of quantitative results) becomes an equally important goal. Reducing variance and improving precision is possibly the most crucial goal as precision helps curtail the number of outliers that inevitably arise due to the stochastic nature of the measurement process.

Received: August 27, 2010
Accepted: December 21, 2010
Published: January 28, 2011

Among quantitative proteomics methods, highest precision can be obtained by techniques using stable isotopes, e.g., stable isotope labeling with amino acids in cell culture (SILAC),[7] absolute quantification (AQUA),[8] quantification concatamers (QconCAT),[9] or equilimolarity through equalizer peptide (EtEP).[10] Chemical labeling of peptides with isotope-coded affinity tags (ICAT)[11] or with isobaric tags such as tandem mass tags (TMT)[12] or isobaric tags for relative and absolute quantitation (iTRAQ)[13] also rely on stable isotopes. Commercially available isobaric tags employ *N*-hydroxy-succinimide (NHS) chemistry to target α- and ε-amino groups. The labels are designed to allow multiplexing of several samples[12−15] by creating peptides of same nominal mass. Characteristic reporter ions are released in tandem mass spectrometry (MS/MS) spectra that can be used for relative quantification. In a recent study, the numbers of identified peptides and proteins were found highest with iTRAQ 4-plex, followed by TMT 6-plex, and lowest with iTRAQ 8-plex; however, the three types of isobaric tags performed similar in terms of quantitative precision and accuracy.[16] Another study indicated that the differences in identification rates depending on the type of isobaric labeling reagent also seemed to apply for phosphopeptides.[17] For quantification of samples labeled with isobaric tags on an LTQ Orbitrap instrument, we and others have shown that acquisition of both a collisionally induced dissociation (CID) and a higher energy collisional dissociation (HCD) scan from each selected precursor combines the sensitivity of CID for identification with the precision of HCD for quantification.[18,19] As the CID scan is acquired using standard settings, the method permits varying the HCD collision energy ad libitum to values optimal for quantification.

A number of studies provide information on the benefits and drawbacks of quantification procedures using isobaric tags including comparisons of various instrument types and methods like pulsed Q collision induced dissociation (PQD) and HCD.[18−27] However, to our knowledge, there have been no reports on the error structure of reporter ion quantification based on HCD spectra acquired on an LTQ Orbitrap XL ETD mass analyzer, which would be interesting in our view as this was the instrument where a new type of HCD cell with an axial extraction field was first implemented. A major problem for quantification using isobaric tags is that the variance of reporter ion areas is not homogeneous, i.e., homoscedastic but heteroscedastic: Several reports have shown that for many types of mass analyzers, the variance increases strongly for precursors that yield only low reporter ion signals.[25−27] Methods have been developed to compensate for heteroscedastic variance by application of a sophisticated error model or variance stabilization transformation.[26,27]

In this report, we examined the precision of HCD-based quantification on an LTQ Orbitrap XL equipped with the original HCD cell as compared to a version of the HCD cell with an axial extraction field that is mounted in Orbitrap XL ETD instruments (Supporting Information, Figure S-1). A similar version of the HCD cell with an axial field is also mounted in Orbitrap Velos instruments.[4] The axial field in the HCD cell was designed to improve ion-optics and fragment ion transmission. We reasoned that it would be interesting to study whether these changes had an impact on the precision of reporter ion quantification. To ensure that small variations in overall instrument performance would be kept to a minimal level, measurements were carried out on one and the same LTQ Orbitrap instrument immediately before and after installation of the HCD cell with the axial field in association with an upgrade for electron transfer dissociation (ETD). Moreover, we also used the same processed samples, the same nano-HPLC equipment, and an identical LC gradient. Experimental samples included both a well-defined mixture of standard proteins in defined ratios and a complex biological sample consisting of a mixture of lysates from two states of HeLa cells (log-phase and nocodazole treated).

EXPERIMENTAL SECTION

Chemicals and reagents, sample preparation, nano-HPLC, mass spectrometry, and data analysis and processing were as described previously.[16] Briefly, two samples A and B were prepared that contained 13 proteins in different ratios. For 7 proteins, the ratio between sample A and B was 1:1, for 3 proteins 5:1, and for 3 other proteins 1:40. The samples were separately digested with trypsin and spiked with synthetic peptides in a ratio between A and B of 1:5. Each of the two samples A and B was then split into two "duplicate" parts and labeled with two different channels of iTRAQ 4-plex reagent, followed by mixing of all four channels. In addition, protein extracts from log-phase vs nocodazole treated HeLa cells were prepared and digested and labeled as follows: Log-phase digests were split into six equal parts and labeled with two channels of iTRAQ 4-plex, TMT 6-plex, and iTRAQ 8-plex reagents respectively, and nocodazole treated digests were split and labeled likewise with two other channels of the respective tags. Three HeLa samples (iTRAQ 4-plex, TMT 6-plex, and iTRAQ 8-plex) were obtained by mixing the four corresponding channels of each type of isobaric tag. In both the protein mix and the HeLa experiments, the variance of duplicate channels from each sample was analyzed and compared. Protein mix samples were analyzed using a 110 min chromatography gradient, whereas HeLa samples were analyzed using a 3.5 h chromatography gradient and gas-phase fractionation. Both a CID scan for identification (automated gain control (AGC) target value 1×10^4, maximum inject time 400 ms, minimum signal threshold 500 counts) and a HCD scan for quantification (AGC target value 3×10^5, maximum inject time 500 ms, minimum signal threshold 500 counts) were acquired for each selected precursor (monoisotopic precursor selection on, rejection of singly charged ions). HeLa data were recorded using 75% normalized collision energy (CE) for HCD, whereas the HCD collision energy was varied as indicated for the experiments using the protein mixture.

The HCD cell with axial field was mounted during upgrade of the LTQ Orbitrap XL instrument to LTQ Orbitrap XL ETD. The HCD cell is a multipole operating according to known principles.[28,29] In the Orbitrap XL ETD and Orbitrap Velos models, there are equally spaced electrodes mounted along the axial direction of the HCD cell that are connected to a resistive divider and that permit the creation of a weak axial extraction field that pushes fragment ions into the C-trap. The axial field was designed to improve ion transmission and reduce fragment ion loss and to speed up the extraction of fragment ions from the HCD cell. Additional details with regard to off-line nanoelectrospray and the comparison between precursor intensity and the sum of all reporter ions are presented in the additional Experimental Section of the Supporting Information.

RESULTS AND DISCUSSION

The primary goal of our study was to test whether a HCD cell with axial field that was designed for the LTQ Orbitrap mass analyzer had an impact on the overall precision of acquired data

and other performance characteristics of HCD-based quantification using isobaric tags.

We first estimated the HCD normalized collision energy (CE%) values at which reporter ion intensities of the three labeling reagents iTRAQ 4-plex, TMT 6-plex, and iTRAQ 8-plex reached a maximum, reasoning that high reporter ion signals potentially help ensure an adequate lower limit of quantification (LLOQ) and high precision. A set of synthetic peptides was derivatized separately with one "channel" of iTRAQ 4-plex, TMT 6-plex, and iTRAQ 8-plex reagents, which cause m/z shifts of 145.1, 229.2, and 304.2, respectively. To plot the relationship between reporter ion intensity and HCD CE%, a mixture containing the three labeled forms of a peptide was analyzed by off-line nanoelectrospray on an LTQ Orbitrap equipped with the original HCD cell (Supporting Information, Figure S-2). Precursor selection was centered on the m/z of the TMT-labeled form, and the isolation window was widened to 100 m/z so that the 4-plex labeled and the 8-plex labeled forms were also isolated. The relative intensities of the three coisolated labeled forms at a HCD collision energy of 0% appeared similar to a MS^1 scan. Subsequently the HCD collision energy was ramped while HCD spectra were recorded. As the labeling reagents were chosen to produce three different types of reporter ions, the relationship between the production of reporter ions and the HCD collision energy could be studied simultaneously. Notably, the optimum reporter ion intensity was found at similar CE% for the three reagents. Reporter ion intensities were found to reach a maximum at a normalized HCD collision energy between 50% and 100%. Interestingly, for 3+ charged precursors, peak reporter ion intensities were observed at a higher normalized collision energy compared to 2+ charged precursors (Supporting Information, Figure S-2). The specific optimum CE% appeared to depend on peptide sequence and charge state, rather than on the type of labeling reagent.

Current LTQ Orbitrap XL ETD and Orbitrap Velos models are equipped with a type of HCD collision cell where an axial field pushes fragment ions into the C-trap. The ion path, axial field, and the electric potential in this HCD collision cell are illustrated schematically in the Supporting Information, Figure S-1. We tested whether the axial field had an impact on performance characteristics such as the precision of reporter ion quantification in HCD scans. We first analyzed a mixture that consisted of two well-defined standard protein and peptide samples A and B (see the Experimental Section). After tryptic digestion, samples A and B were split and each was labeled with two different channels of iTRAQ 4-plex reagent followed by mixing of all four channels. Therefore the theoretical ratios of duplicate channels were 1:1. In this way, an alteration of the dispersion of duplicate channel ratios could serve as an indicator of differences in the overall precision of the acquired data, a measure of data quality. The sample was first analyzed on an LTQ Orbitrap equipped with the original HCD cell. After exchange of the HCD cell, the sample was analyzed again on the same instrument equipped with a HCD cell with an axial field and the results were compared. All measurements were accomplished with the recently described CID-HCD method.[18,19] This method permits a variation of the HCD collision energy as HCD scans are used only for quantification. Figure 1A shows that for all tested HCD collision energy settings, the percentage of HCD spectra where one or more reporter ions failed to be detected was strongly reduced with the HCD collision cell with an axial field (paired t test $p < 0.0001$). The axial field decreased the average percentage of such spectra from ~25% to ~2.5%. This suggests that the lower limit of quantification (LLOQ) is closer to the lower limit of detection (LLOD) for data acquired with the axial field as compared to the original HCD cell. In addition, quantification using the HCD cell with an axial field was associated with improved precision as illustrated by a smaller geometric standard deviation of duplicate channel ratios, and this effect was consistent over the entire range of tested collision energies (Figure 1B,C). In absolute terms, the geometric standard deviation was higher for duplicate channel ratios derived from reporter ion areas 115 and 114, which contained three proteins that were diluted 1:40-fold in relation to channels 117 and 116 (the largest ratio in this experiment). This suggests that quantification of peptides with large ratios between the channels can lead to higher variance in the channels containing the smaller reporter ion area values, which is in accordance with reported observations.[24] On average, the axial field decreased the geometric standard deviation of duplicate channel ratios 115:114 from 1.25 to 1.15 (paired t test $p < 0.014$) and of duplicate channel ratios 117:116 from 1.13 to 1.07 ($p < 0.014$). We observed a correlation between the sum of all reporter ion areas and the intensity of the corresponding parent precursor ion as illustrated in a log−log graph (Supporting Information, Figure S-3). This suggests that the ratio of these two quantities, calculated as the median over many peptide-spectrum matches, could provide an estimate of which fraction of the precursor ion current can be detected as reporter ion currents. We therefore calculated the percentage of the sum of the reporter areas divided by the respective parent precursor intensity (see additional Experimental Section in the Supporting Information for details and justification) and determined the median thereof for each run. Interestingly, this percentage value correlated with the observed precision and with the fraction of HCD spectra with a complete set of reporter ions. Moreover these percentage values were significantly higher when a HCD cell with axial field was used (Figure 1D). This suggests that the axial field indeed improved reporter ion transmission significantly, most likely by reducing the loss of reporter ions. In summary, both the percentage of HCD spectra with full quantitative information and the precision of quantification improved using a HCD cell with axial field, and these improvements could be noticed over the entire range of tested collision energies (CE 45% to CE 105%).

We further monitored whether improved precision could also be observed upon analysis of a complex biological sample and whether the effect was consistent when other isobaric labeling reagents were employed in addition to iTRAQ 4-plex. Protein extracts from the log-phase and nocodazole treated HeLa cells were digested with trypsin and split followed by labeling with iTRAQ 4-plex, TMT 6-plex, and iTRAQ 8-plex, respectively, as described in the Experimental Section. Again the variation of duplicate channel ratios was compared. All samples were first analyzed using the original HCD cell. After exchange of the HCD cell, samples were analyzed again using the HCD cell with axial field. Percentiles of duplicate channel ratios were plotted (Supporting Information, Figure S-4) showing once more that the axial field improved analytical precision. In addition, the improvement was found consistent for all three types of isobaric labeling reagents.

Data from the HeLa iTRAQ 4-plex measurements acquired with the original HCD cell and the HCD cell with an axial field, respectively, were visualized in a way similar to MA-plots of RNA microarray studies[30] where regulatory ratios are plotted against

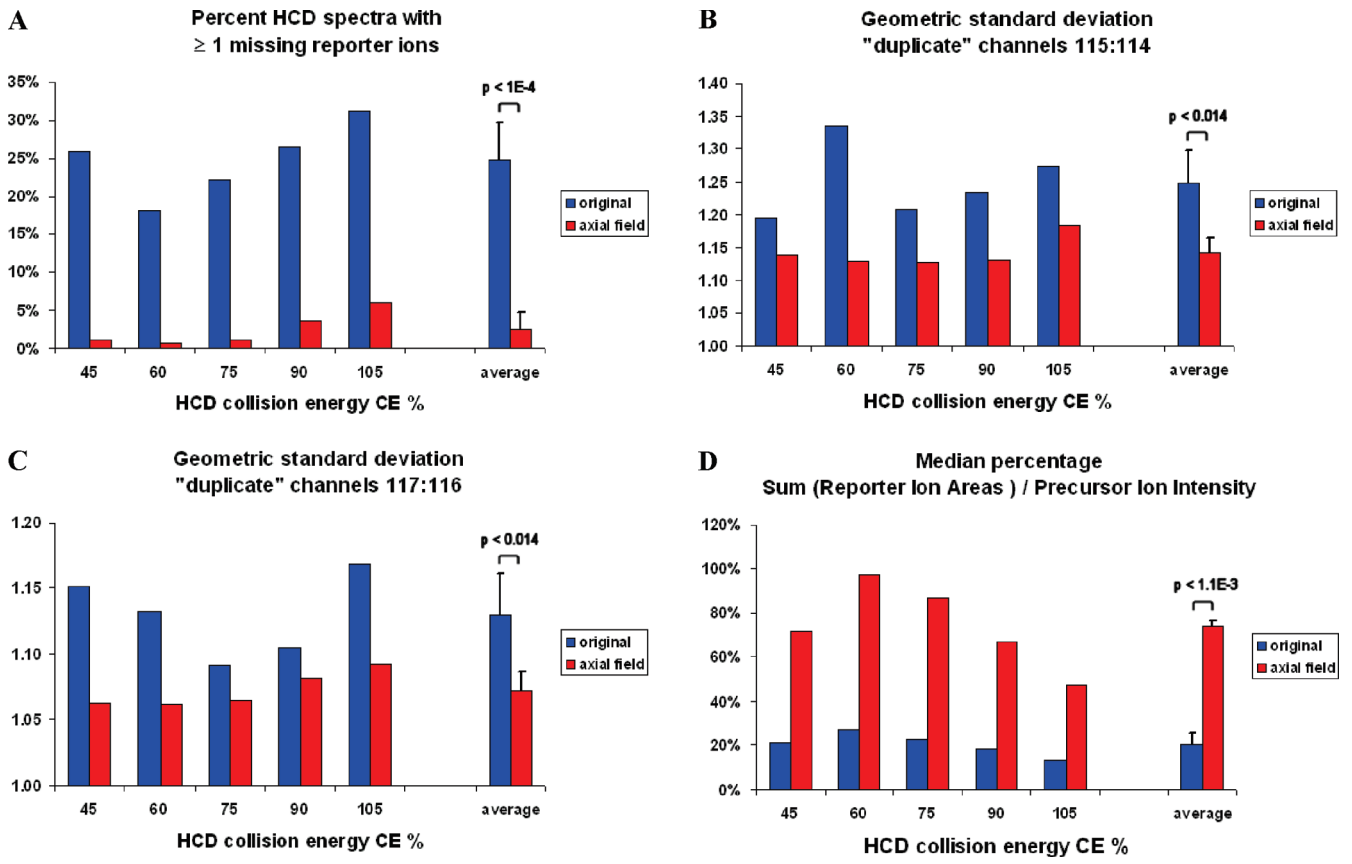

Figure 1. A HCD cell with an axial field decreases the fraction of HCD spectra with missing reporter ions and improves analytical precision. Analysis of a standard protein mixture on an LTQ Orbitrap equipped with the original HCD cell as compared to a HCD cell with an axial field. Panel A indicates the percentage of HCD spectra where one or more reporter ions failed to be detected. The geometric standard deviation of "duplicate" channels is depicted in panel B (for the ratio 115:114) and panel C (for the ratio 117:116). Panel D shows the fraction of the precursor ion currents that can be detected as reporter ion currents, as a measure of fragment ion generation and transmission. In each panel (A−D) individual measurements are shown on the left side, whereas arithmetic averages with one-sided error bars denoting 1 SD are shown on the right side. *p*-values calculated as a 2-sided paired *t* test for the comparison of the original HCD cell vs the HCD cell with an axial field.

signal intensities as log−log graphs. Such plots allow a rapid visual inspection of global or intensity-dependent bias which would become evident as an asymmetric distribution or as a skewing or curvature of the scatter-plot data. Most important, the dispersion of duplicate channel ratios can highlight patterns of intensity-dependent differences in analytical precision. In the plots shown in Figure 2, each dot represents a peptide-spectrum match. Figure 2A depicts an overlay of the results of measurements with the original HCD cell (in blue) as compared to the HCD cell with an axial field (in red). In this plot, the *x*-axis represents $\log_2$ of the geometric mean of reporter ion areas 114 and 115 while the *y*-axis represents $\log_2$ of duplicate channel ratios 115:114 (split nocodazole sample). The higher variance of duplicate channel ratios derived from low reporter ion areas becomes apparent in Figure 2A as a funnel-like dispersion pattern of data points, reflecting an inverse relationship between the mean reporter ion area (signal strength) and precision, i.e., heteroscedastic variance. As compared to the original HCD cell (blue data points), reporter areas were shifted to higher values for data acquired using the HCD cell with an axial field (red data points); thus, the intensity-dependent decrease in analytical precision associated with low reporter ion areas appeared less prominent.

For the plot shown in Figure 2B, the *y*-axis values depict once again the variation of $\log_2$ duplicate channel ratios 115:114 from the HeLa 4-plex experiments. However, for this plot the *x*-axis values reflect the percentile rank ordered by the geometric mean of the respective reporter ion channel areas. The advantage of this form of data visualization is that data points are distributed evenly along the *x*-axis.[27] The plot illustrates high overall precision of a large percentage of data points when using a HCD cell with an axial field (red) as compared to the original HCD cell (blue). Figure S-5 in the Supporting Information is analogous to Figure 2; however, in the former figure the *x*-axis reflects either precursor intensity (Supporting Information, Figure S-5A) or percentile rank ordered by precursor intensity (Supporting Information, Figure S-5B). These plots suggest that analytical precision is maintained for a broad range and a broad fraction of precursor intensities when using a HCD cell with an axial field.

Summing up, we have shown that a HCD fragmentation cell with an axial electric field leads to an improvement of several important performance characteristics upon HCD-based quantification of peptides labeled with isobaric tags, most notably improved overall data precision and a higher percentage of HCD spectra with a complete set of reporter ions. The original HCD cell of our LTQ Orbitrap XL instrument was exchanged for a version with an axial field upon upgrade to an LTQ Orbitrap XL ETD, permitting an examination of the direct effect of the

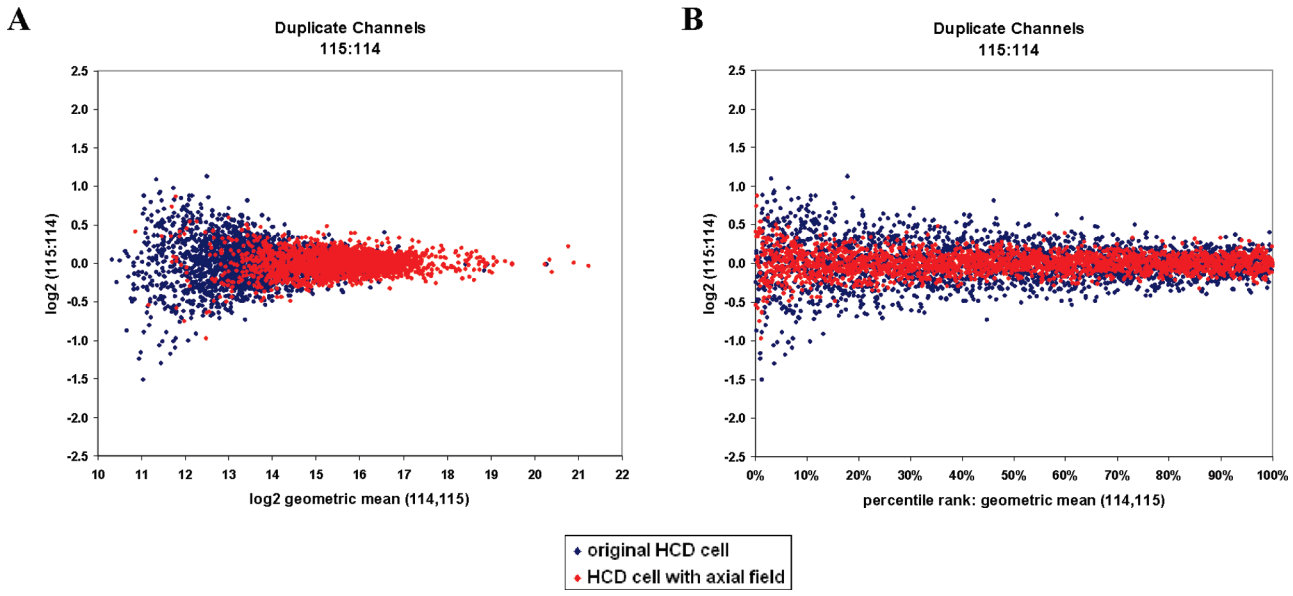

Figure 2. The axial field improves reporter ion transmission, thereby increasing the overall precision of data acquired with the axial field. Scatter plots illustrating the variation of duplicate channel ratios in relation to reporter ion signals. Each data point represents a peptide-spectrum match. The $\log_2$ of duplicate channel ratios on the *y*-axis is plotted against a measure of reporter ion signal intensity. In panel A the *x*-axis is proportional to the $\log_2$ of the geometric mean of reporter ion areas 114 and 115, whereas in panel B it is proportional to the rank of the mean thus ensuring an even distribution of data points along the *x*-axis. Data are from the analyses of the iTRAQ 4-plex labeled HeLa sample (nocodazole sample split before labeling). Precision is high where the dispersion of the data points is narrow.

exchange of the HCD cell. A HCD cell with an axial field is also mounted in LTQ Orbitrap Velos models. However, several alterations were introduced with this new generation of LTQ Orbitrap instruments including a stacked ring ion guide ("S-lens"), a dual-pressure ion trap, and a direct connection of the HCD cell to the C-trap in the form of an integrated C-trap/HCD collision cell combination,[4] which would make it difficult to discern the contribution of the axial field alone. We believe that the increased precision observed using a HCD cell with an axial field is indeed significant. Since the improvements seem to hold for a broad dynamic range including low intensity precursors, we feel that the benefits of the axial field are specifically useful for an analysis of complex samples. Further results and discussion with regard to the relevance of these results can be found in the Supporting Information.

As Figure 2A illustrates, reporter ion areas were generally shifted to higher values with the HCD cell with an axial field. Together with Figure 1D, this observation suggests that the observed overall improvement in the precision of acquired data is probably a consequence of improved ion transmission resulting in better ion statistics due to an increased number of ions that are quantifiable with higher precision. It should be noted that all data were acquired using automatic gain control (AGC), which ensures that less abundant, low intensity precursor ions are accumulated in the LTQ ion trap for a proportionally longer inject time (fill time) prior to fragmentation in the HCD cell (as long as the limit set by the maximum inject time is not reached). In this way automatic gain control helps ensure adequate signal strength for low intensity precursor ions. This interpretation is supported by scatter plots that display the relationship between duplicate channel ratios and precursor ion intensities (see the Supporting Information, Figure S-5). The prolonged accumulation of low intensity precursor ions for MS^2 analysis due to automatic gain control might therefore constitute an advantage over MS^1-based quantification methods such as label-free or SILAC dependent approaches. For instance, with SILAC quantification, coeluting ions influence the inject time of MS^1 scans, and with label-free quantification such as selective reaction monitoring (SRM), the dwell time is either fixed or depends on the number of other transitions monitored at the same time ("scheduled SRM"). In both situations, there is usually no prolonged measurement time or compensatory accumulation of low-intensity signals. In summary, iTRAQ quantification on the HCD cell with an axial field combined with automatic gain control showed acceptable precision over a broad range of precursor ion intensities. Remarkably, with our test sample the complete set of reporter ions was detected in almost all (~97.5%) HCD spectra for which the corresponding CID spectrum led to a peptide identification, as compared to only ~75% with the original HCD cell. This suggests that for quantification using isobaric tags, the lower limit of quantification (LLOQ) is closer to the lower limit of detection (LLOD) for data acquired with the axial field as compared to the original HCD cell.

CONCLUSIONS

An axial electric field in the HCD collision cell of the LTQ Orbitrap improves ion transmission of reporter ions, thereby increasing the overall precision of quantification using isobaric tags. The improvements were consistent for all three types of isobaric labeling reagents that we tested (iTRAQ 4-plex, TMT 6-plex, and iTRAQ 8-plex). Notably, analytical precision remained adequately high even for quantification based on precursor ions of low intensity. We consider analytical precision one of the most critical factors in quantitative proteomics, as it controls both the number of outliers, i.e., the false discovery rate (FDR) with regard to quantification, and the statistical power of a study, i.e., the chance of a study to detect truly regulated proteins. In addition, the axial field led to an increase in the fraction of HCD spectra in which the complete set of reporter ions could be

detected. We conclude that the HCD collision cell with axial field makes the LTQ Orbitrap well suited for quantitative shotgun proteomics using isobaric tags. The precision of data obtained even for low intensity precursors establishes HCD-based quantification as a competitive approach for quantitative shotgun "precision proteomics".[31] We hope that our findings may help researchers in their design of quantitative proteomics studies using isobaric tags.

■ ASSOCIATED CONTENT

Supporting Information. Additional figures and table and additional experimental section and discussion. This material is available free of charge via the Internet at http://pubs.acs.org.

■ AUTHOR INFORMATION

Corresponding Author

*Address: Christian Doppler Laboratory for Proteome Analysis, Dr. Bohr-Gasse 3, 1030 Vienna, Austria. E-mail: pichler@imp.univie.ac.at. Phone: +43-1-79044-4293. Fax: +43-1-79044-110.

■ ACKNOWLEDGMENT

We are grateful to Dr. Karin Grosstessner-Hain (IMP) for preparation of the HeLa cell extracts and to Dr. Ilse Dohnal (CD-Laboratory for Proteome Analysis) and Dr. James Hutchins (IMP) for useful discussions and critical reading of the manuscript. The authors also wish to thank Dr. Stevan Horning and Dr. Alexander Makarov (Thermo Scientific) for useful advice and discussion. Dr. Peter Pichler wishes to dedicate his contribution to his father Dr. Horst Pichler for encouraging his interest in science. This work was supported by the Christian Doppler Research Association CDG (Christian Doppler Forschungsgesellschaft) and by the Austrian Proteomics Platform (APP-III) within the Austrian Genome Research Program (GEN-AU). Dr. Johann Holzmann and Prof. Dr. Gustav Ammerer were supported by the Austrian Science Foundation FWF (Fonds zur Förderung der wissenschaftlichen Forschung), Grant SFB-F34.

■ REFERENCES

(1) Han, X.; Aslanian, A.; Yates, J. R., 3rd. *Curr. Opin. Chem. Biol.* **2008**, *12*, 483–490.
(2) Wilm, M.; Shevchenko, A.; Houthaeve, T.; Breit, S.; Schweigerer, L.; Fotsis, T.; Mann, M. *Nature* **1996**, *379*, 466–469.
(3) Cox, J.; Mann, M. *Nat. Biotechnol.* **2008**, *26*, 1367–1372.
(4) Olsen, J. V.; Schwartz, J. C.; Griep-Raming, J.; Nielsen, M. L.; Damoc, E.; Denisov, E.; Lange, O.; Remes, P.; Taylor, D.; Splendore, M.; Wouters, E. R.; Senko, M.; Makarov, A.; Mann, M.; Horning, S. *Mol. Cell. Proteomics* **2009**, *8*, 2759–2769.
(5) Ong, S. E.; Mann, M. *Nat. Chem. Biol.* **2005**, *1*, 252–262.
(6) Gstaiger, M.; Aebersold, R. *Nat. Rev. Genet.* **2009**, *10*, 617–627.
(7) Ong, S. E.; Mann, M. *Nat. Protoc.* **2006**, *1*, 2650–2660.
(8) Gerber, S. A.; Rush, J.; Stemman, O.; Kirschner, M. W.; Gygi, S. P. *Proc. Natl. Acad. Sci. U.S.A.* **2003**, *100*, 6940–6945.
(9) Beynon, R. J.; Doherty, M. K.; Pratt, J. M.; Gaskell, S. J. *Nat. Methods* **2005**, *2*, 587–589.
(10) Holzmann, J.; Pichler, P.; Madalinski, M.; Kurzbauer, R.; Mechtler, K. *Anal. Chem.* **2009**, *81*, 10254–10261.
(11) Gygi, S. P.; Rist, B.; Gerber, S. A.; Turecek, F.; Gelb, M. H.; Aebersold, R. *Nat. Biotechnol.* **1999**, *17*, 994–999.
(12) Thompson, A.; Schafer, J.; Kuhn, K.; Kienle, S.; Schwarz, J.; Schmidt, G.; Neumann, T.; Johnstone, R.; Mohammed, A. K.; Hamon, C. *Anal. Chem.* **2003**, *75*, 1895–1904.
(13) Ross, P. L.; Huang, Y. N.; Marchese, J. N.; Williamson, B.; Parker, K.; Hattan, S.; Khainovski, N.; Pillai, S.; Dey, S.; Daniels, S.; Purkayastha, S.; Juhasz, P.; Martin, S.; Bartlet-Jones, M.; He, F.; Jacobson, A.; Pappin, D. J. *Mol. Cell. Proteomics* **2004**, *3*, 1154–1169.
(14) Dayon, L.; Hainard, A.; Licker, V.; Turck, N.; Kuhn, K.; Hochstrasser, D. F.; Burkhard, P. R.; Sanchez, J. C. *Anal. Chem.* **2008**, *80*, 2921–2931.
(15) Choe, L.; D'Ascenzo, M.; Relkin, N. R.; Pappin, D.; Ross, P.; Williamson, B.; Guertin, S.; Pribil, P.; Lee, K. H. *Proteomics* **2007**, *7*, 3651–3660.
(16) Pichler, P.; Kocher, T.; Holzmann, J.; Mazanek, M.; Taus, T.; Ammerer, G.; Mechtler, K. *Anal. Chem.* **2010**, *82*, 6549–6558.
(17) Thingholm, T. E.; Palmisano, G.; Kjeldsen, F.; Larsen, M. R. *J. Proteome Res.* **2010**, *9*, 4045–4052.
(18) Zhang, Y.; Ficarro, S. B.; Li, S.; Marto, J. A. *J. Am. Soc. Mass Spectrom.* **2009**, *20*, 1425–1434.
(19) Kocher, T.; Pichler, P.; Schutzbier, M.; Stingl, C.; Kaul, A.; Teucher, N.; Hasenfuss, G.; Penninger, J. M.; Mechtler, K. *J. Proteome Res.* **2009**, *8*, 4743–4752.
(20) Gan, C. S.; Chong, P. K.; Pham, T. K.; Wright, P. C. *J. Proteome Res.* **2007**, *6*, 821–827.
(21) Griffin, T. J.; Xie, H.; Bandhakavi, S.; Popko, J.; Mohan, A.; Carlis, J. V.; Higgins, L. *J. Proteome Res.* **2007**, *6*, 4200–4209.
(22) Bantscheff, M.; Boesche, M.; Eberhard, D.; Matthieson, T.; Sweetman, G.; Kuster, B. *Mol. Cell. Proteomics* **2008**, *7*, 1702–1713.
(23) McAlister, G. C.; Phanstiel, D.; Wenger, C. D.; Lee, M. V.; Coon, J. J. *Anal. Chem.* **2010**, *82*, 316–322.
(24) Ow, S. Y.; Salim, M.; Noirel, J.; Evans, C.; Rehman, I.; Wright, P. C. *J. Proteome Res.* **2009**, *8*, 5347–5355.
(25) Kuzyk, M. A.; Ohlund, L. B.; Elliott, M. H.; Smith, D.; Qian, H.; Delaney, A.; Hunter, C. L.; Borchers, C. H. *Proteomics* **2009**, *9*, 3328–3340.
(26) Zhang, Y.; Askenazi, M.; Jiang, J.; Luckey, C. J.; Griffin, J. D.; Marto, J. A. *Mol. Cell. Proteomics* **2010**, *9*, 780–790.
(27) Karp, N. A.; Huber, W.; Sadowski, P. G.; Charles, P. D.; Hester, S. V.; Lilley, K. S. *Mol. Cell. Proteomics* **2010**, *9*, 1885–1897.
(28) Paul, W. *Rev. Mod. Phys.* **1990**, *62*, 531–540.
(29) Schwartz, J. C.; Senko, M. W.; Syka, J. E. *J. Am. Soc. Mass Spectrom.* **2002**, *13*, 659–669.
(30) Dudoit, S.; Yang, Y. H.; Callow, M. J.; Speed, T. P. *Stat. Sin.* **2002**, *12*, 111–139.
(31) Mann, M.; Kelleher, N. L. *Proc. Natl. Acad. Sci. U.S.A.* **2008**, *105*, 18132–18138.